

## *Ipomoea quamoclit* L. Leaf Extract Assisted Synthesis of Silver Nanoparticles: Study of its Application on Catalytic Degradation of Dyes and Antibacterial Efficacy

ABIRAMI AKKINIRAJ CHANDRASEKAR<sup>ID</sup> and PANDIAN KANNAIYAN<sup>\*ID</sup>

Department of Inorganic Chemistry, University of Madras, Guindy Campus, Chennai-600025, India

\*Corresponding author: E-mail: jeevapandian@yahoo.co.uk

Received: 23 February 2022;

Accepted: 23 April 2022;

Published online: 18 July 2022;

AJC-20889

Recently nanoparticles have been widely used in various applications such as antimicrobial, drug delivery, catalysis, sensors and screening of toxic organic and inorganic pollutants. Here we present an environmentally friendly, simple approach and an efficient approach for the green synthesis of silver nanoparticles using *Ipomoea quamoclit* L. leaf extract. In this work, a novel method for green synthesis of silver nanoparticles-based *Ipomoea quamoclit* L. plant extract as green reducing agent is described. The morphological and optical properties of the nanoparticles were characterized by XRD, FT-IR, HR-SEM, TEM and UV-visible spectrum. The silver nanoparticles prepared from *Ipomoea quamoclit* L. had a size range from 20 nm to 50 nm as observed by the FE-SEM analysis. The XRD pattern revealed the crystallinity nature of the prepared silver nanoparticles. Stable silver nanoparticle solution has been synthesized using *Ipomoea quamoclit* L. leaf extract under the optimized experimental conditions. This silver nanoparticle can be used as a catalyst for degradation of textile dyes. The resulting reaction follows pseudo-first-order kinetics. The silver nanoparticles exhibited a moderate antibacterial activity towards *Bacillus subtilis* and *Salmonella* sp. had an inhibition zone of 34 mm and 20 mm, respectively.

**Keywords:** Silver nanoparticles, *Ipomoea quamoclit* L., Antibacterial activity, Green synthesis.

### INTRODUCTION

Nanoparticles exhibited unique morphology, size and shape because of distinct properties of large surface-to-volume ratio [1-3]. Metal nanoparticles have been used for various applications in pharmaceutical, sensor, agriculture and catalytic applications [4-6]. Nanoparticles synthesized through the conventional techniques (physical and chemical method) use a facial method to synthesize nanoparticles in large quantity however, the chemical synthesis requires toxic chemicals as reducing agent as well as stabilizing agents for synthesis materials [7,8].

Nanoparticles like Au, Ag, Cu, Fe, and Se have been used for various academic and industrial applications [9,10]. Silver nanoparticles (AgNPs) are a well-known material for antibacterial and wound healing is well established [11,12]. Moreover, due to release of silver ion (Ag<sup>+</sup>) from AgNPs inhibits respiratory enzymes and produces ROS (reactive oxygen species), therefore they are in high demand in medicine, cleaning agents, food stuff and consumer products.

Metal nanoparticles with different size and shapes can be synthesized by various experimental conditions including chemical reduction, polyol method, microwave synthesis, sonochemical, electrochemical and photochemical, etc. [13,14]. Recently, green chemistry method is one of the fascinating areas of research on the synthesis of various types of size and differently shaped metal nanoparticles. Some of the medicinal plants like aloe vera gel have been used for the synthesis of stabilized silver nanoparticles [15]. In conventional process, high temperatures, reduction of silver ions in solution media (sodium borohydride) and capping agents (gelatine) were used for the reduction of silver ions. Green synthesis using plant extract as a rich source of capping agents and reducing agents could be a potential candidate for the synthesis of silver nanoparticles [16].

*Ipomoea quamoclit* L., genus belongs to the Convolvulaceae family and is also called as *Quamoclit pinnata*. *Ipomoea quamoclit* L., is commonly known as star glory, cardinal vine, Indian pink and moreover, it is the most important herb in folk and Ayurveda medicine. Its stems and leaves contain alkaloids and cyanogenetic glycosides. Plant leaves were used to stop

bleeding piles and carbuncles. *Ipomoea quamoclit* L. plant possesses many medicinal properties such as anticancer, anti-diabetic, antimicrobial, and antioxidant activity [17,18]. Recently some of the preliminary studies on the synthesis of silver nanoparticles has been reported using *Ipomoea quamoclit* L. leaf extract, however not much information is given in that study [19]. The objective of the present work is to synthesize silver nanoparticles using *Ipomoea quamoclit* L. leaf extract and then evaluate the antibacterial and catalytic effect of silver nanoparticles.

## EXPERIMENTAL

The *Ipomoea quamoclit* L. plant was collected from in and around Chengalpattu near Chennai, India and authenticated by the Botanist of University of Madras, Chennai, India. Silver nitrate ( $\text{AgNO}_3$ ) was obtained from SRL Chemicals, Chennai, India and used as received. Other solvents of analytical grade were received from the reputed commercial sources.

**Preparation of *Ipomoea quamoclit* L. leaf extract:** The collected *Ipomoea quamoclit* L. leaf was washed with sterilized distilled water to remove the dust particles. The clean leaves were shade dried and then crushed well into a powder form using agate mortar. About 10 g of powder was dispersed in 100 mL of distilled water, then the solution was heated to 60 °C in the water bath for 15 min. Finally, the extract was filtered, collected and stored at 5 °C under dark until further use.

**Synthesis of silver nanoparticles:** To synthesize AgNPs, different volume of the *Ipomoea quamoclit* L. leaf extract was added into the known volume of  $\text{AgNO}_3$  (1 mM) solution. The reaction mixture was placed at room temperature for 24 h and then recorded the absorbance using UV-Spectrum to confirm the formation of AgNPs.

**Characterization:** The optical absorption spectrum was analyzed using UV-visible spectrophotometer (Shimadzu, U-1800). The XRD pattern of AgNPs was recorded using the X-ray instrument Shimadzu XRD-6000 diffractometer. An Infrared spectrum was recorded using Perkin-Elmer 360 spectrophotometer. Morphological and structural investigations were carried out with HR-SEM, Thermoscientific Apero S and HR-TEM, JEM-2100 Plus instrument, Japan.

**Screening of antibacterial activity:** The antibacterial activity of silver nanoparticles was carried out based on the agar disc diffusion method using Muller-Hinton agar (MHA) [20]. Stock cultures were maintained at 4 °C in the Nutrient agar medium. Active cultures for experiments were prepared by transferring a loop full of culture from the stock cultures into the test tubes containing nutrient broth, which was incubated for 24 h at 37 °C. Muller-Hinton agar (MHA) medium was poured into the Petri plate. After the medium was solidified, the inoculums were spread on the solid plates with sterile swabs moistened with the bacterial strains placed in the disc. Ampicillin 20  $\mu\text{L}$ /disc was used as control antibiotics for this study.

## RESULTS AND DISCUSSION

**UV-visible spectra:** The growth of the synthesized silver nanoparticles was monitored using UV-visible spectral studies by monitoring the increase of the SPR band at around 420 nm at different time intervals. With the help of UV-visible spectral

studies, it is possible to optimize the amount of reducing agent required for the complete reduction in various time intervals. The rate of reduction of  $\text{AgNO}_3$  after the addition of 0.5 mL of *Ipomoea quamoclit* L. leaf extract was monitored by measuring the increase in absorbance values at different time scales. It is understood that initially, the reaction is slow and then increased slowly with reaction time. The growth kinetic of AgNPs is shown in Fig. 1 and found that the reaction completed within 24 h. The influence of *Ipomoea quamoclit* L. leaf extract quantity on the reduction of  $\text{AgNO}_3$  was investigated. Different proportion of *Ipomoea quamoclit* L. leaf extract was mixed with a fixed concentration of  $\text{AgNO}_3$  and then allowed to stand for overnight in order to attain complete reduction of  $\text{AgNO}_3$  under dark condition. The UV-visible spectrum of each reaction mixture was recorded and the data are presented in Fig. 2. The AgNPs gave the sharp intensity peak at 420 nm as shown in Fig. 2. It is inferred that when increasing the *Ipomoea quamoclit* L. leaf extract concentration from 0.1 to 1.0 mL, the absorbance values also increase. In addition, the synthesis of AgNPs has been carried out at room temperature at pH 9. It is well known that AgNPs exhibit reddish yellow colour due to the excitonic vibration electron due to the surface plasmon resonance (SPR) of AgNPs. The biosynthesis of AgNPs was performed at room temperature for 24 h. The colour of the solution was stable for about one month and then slowly colour changed from orange-yellow to grey colour. In conclusion, the *Ipomoea quamoclit* L. leaf extract exhibit a very good reducing agent as well as a stabilizing agent. The present method is considered to be one of the easy ways to synthesis AgNPs in the biogenic approach. The formation of AgNPs was confirmed from UV-vis analysis and observed that some antioxidant and bioactive molecules present in the plant extract are responsible for the reduction of  $\text{Ag}^+$  to AgNPs (Fig. 3). The different pH ranges of plant extract for the formation of silver nanoparticles were studied and found that pH 9 stable silver nanoparticles were formed (Fig. 4). In general, the biogenic approach of the presence of polyphenol and flavonoids in the plant extract is responsible for the silver

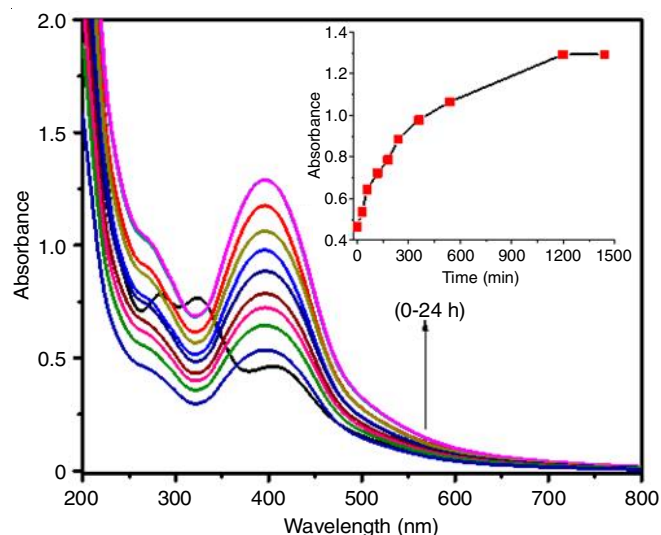


Fig. 1. Time evolution of UV-visible spectrum during the formation of silver nanoparticles from *Ipomoea quamoclit* L. leaf extract (insert: plot of time vs. absorbance)

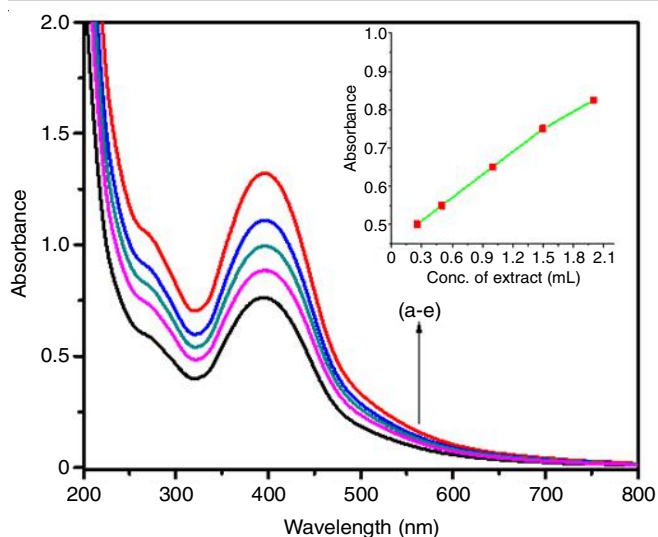


Fig. 2. UV-visible spectrum of the formation of silver nanoparticles from different concentrations of *Ipomoea quamoclit* L. leaf extract (insert: plot of different concentration vs. absorbance)

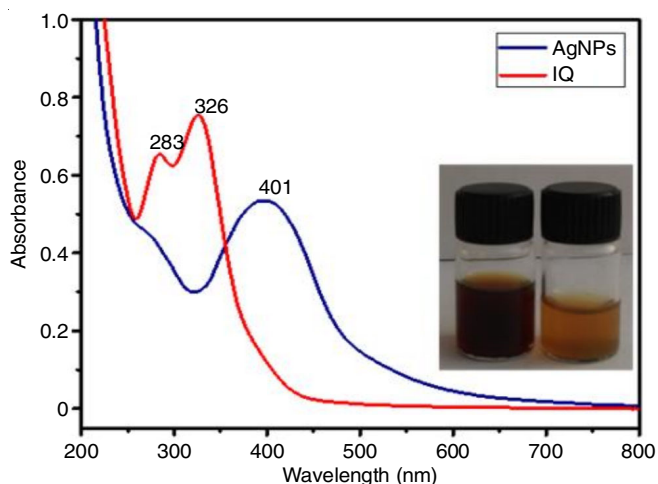


Fig. 3. UV-visible spectrum of the formation of silver nanoparticles from *Ipomoea quamoclit* L. leaf extract (insert: colour picture of silver nanoparticle formed and extract)

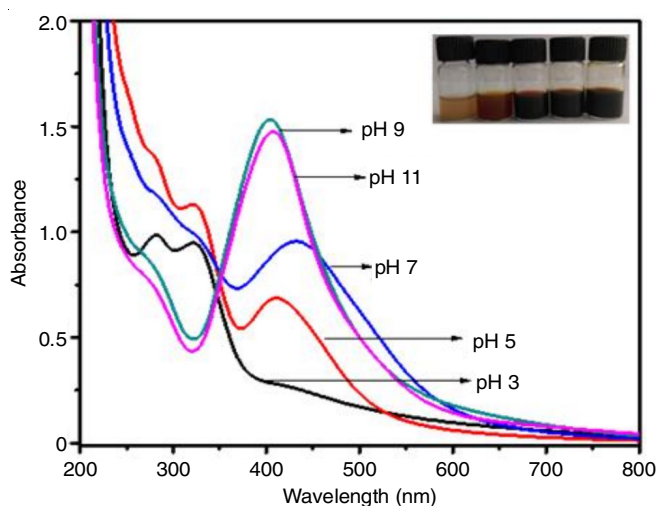


Fig. 4. UV-visible spectrum of the formation of silver nanoparticles from different pH of *Ipomoea quamoclit* L. leaf extract (insert: colour picture of silver nanoparticle formed at diff pH)

nanoparticles formation and also the unreacted flavonoid and polyphenol play a vital role to stabilize silver nanoparticles against aggregation.

**XRD spectra:** Fig. 5 shows the XRD pattern of green synthesized silver nanoparticles. The diffraction peaks pattern observed at  $2\theta$  values of  $38.10^\circ$ ,  $44.30^\circ$ ,  $66.40^\circ$  and  $75.50^\circ$ , which correspond to (111), (200), (220) and (311) plane, respectively. These peaks are consistent with fcc (face-centered cubic) phase of silver nanoparticles (JCPDS file no: 04-0783) [21-22]. The particle size of green synthesized silver nanoparticles can be calculated by using the Debye-Scherrer's formula [23] and the observed mean crystalline size of silver nanoparticles was found to be  $\approx 32$  nm.

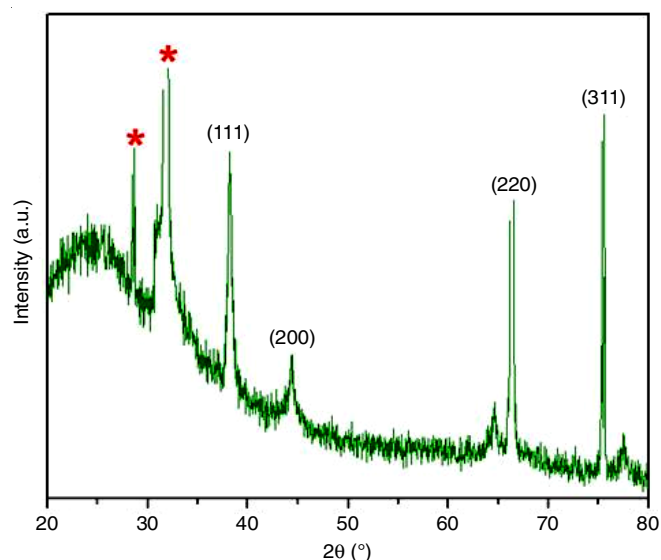


Fig. 5. XRD analysis of silver nanoparticles using *Ipomoea quamoclit* L.

**Surface characterization:** Fig. 6a-b show the HR-SEM images of silver nanoparticles with different magnifications and observed that the particles are spherical in nature with agglomeration between the particles was observed for the synthesized silver nanoparticles. To obtain more information of size and shape for the individual nanoparticles dispersed samples can be used.

Fig. 6c depicted the TEM images of the synthesized silver nanoparticles obtained by the biogenic approach. The particles are almost spherical in shape with average size ranges of 20-30 nm. To measure the chemical composition of the synthesis of the silver nanoparticles by this method and the percentage of silver present in the sample can be measured by energy-dispersive X-ray spectroscopy as shown in Fig. 6d. The EDX spectrum clearly shows the presence of silver nanoparticles without any other major impurities. In addition, a trace amount of some of the elements such as oxygen and carbon are present in the sample, which is due to the coexistence of the capping agents

**FT-IR studies:** FT-IR was employed to investigate the possible biomolecules efficient stabilization and responsible for capping of the green synthesized silver nanoparticles. Fig. 7 represents the FT-IR spectra of the silver nanoparticles. The FT-IR absorbance peaks appeared at  $3090$ ,  $2320$ ,  $1452$ ,  $1312$ ,  $1158$ ,  $1290$ ,  $820$ , and  $492$   $\text{cm}^{-1}$ , which evidenced the nature of

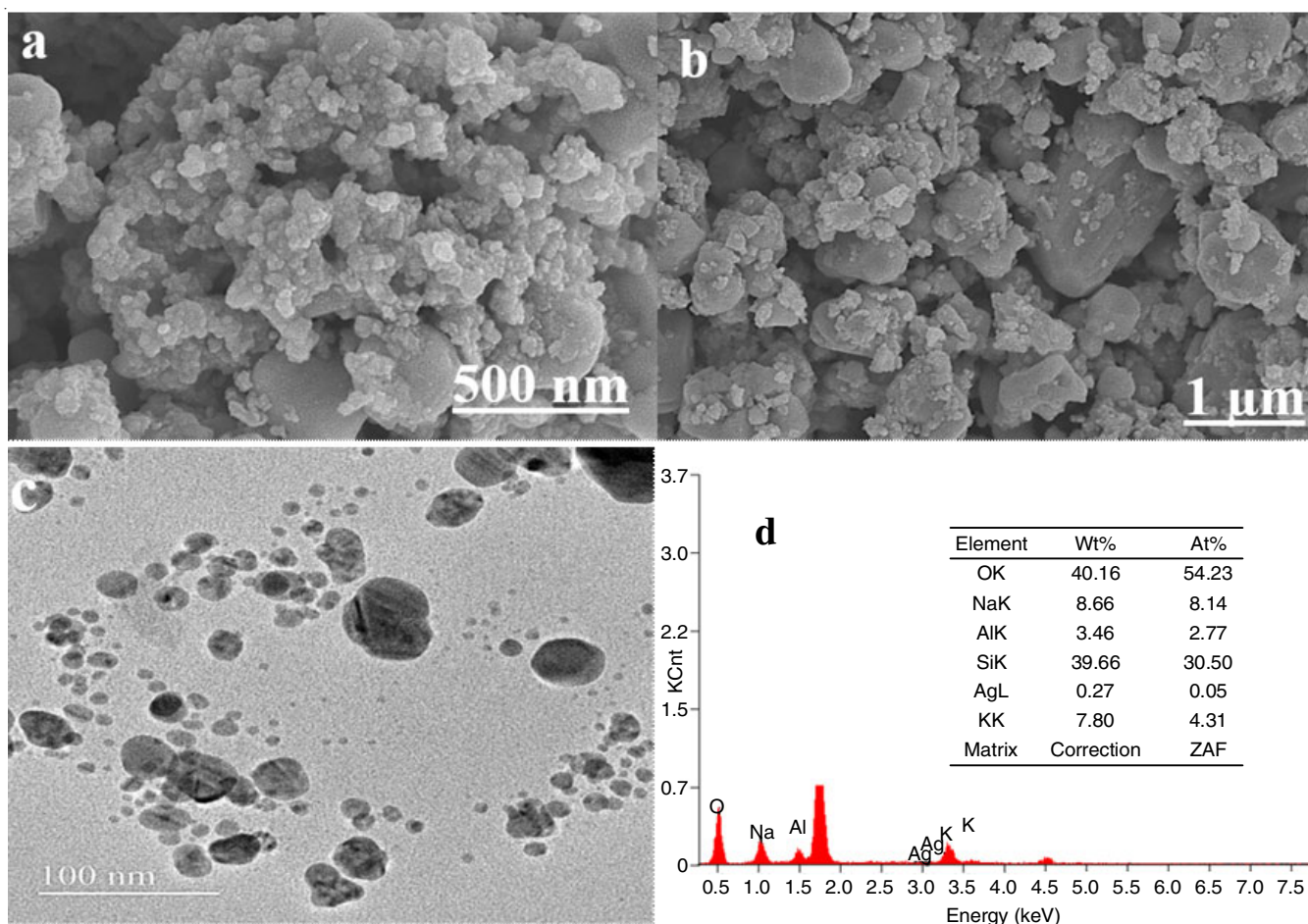


Fig. 6. HR-SEM images of *Ipomoea quamoclit* L. extract synthesized silver nanoparticles in different magnifications (a&b), TEM image (c) and EDAX spectrum (d)

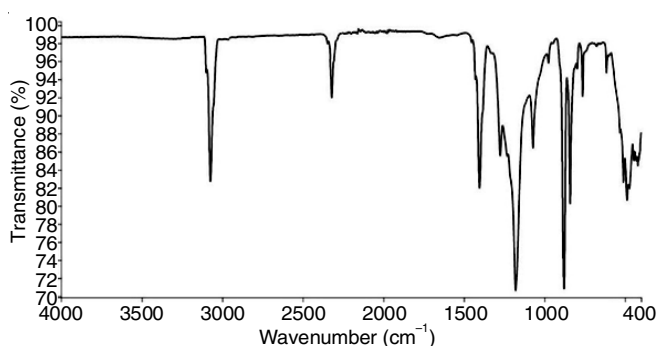


Fig. 7. FT-IR spectra of silver nanoparticles formed using *Ipomoea quamoclit* L

the stabilizing agent and the mode of binding with silver nanoparticles. The appearance of a peak at  $3090\text{ cm}^{-1}$  corresponds to O-H stretching, which is due to the existence of phenol and alcohol molecules present in the sample [24]. A peak at  $2320\text{ cm}^{-1}$  is assigned for the presence of  $\text{CH}_2$  stretching vibration and another peak at  $1452\text{ cm}^{-1}$  is due to the amide band and also for C=C stretching [25]. A peak at  $1312\text{ cm}^{-1}$  is attributed to the symmetrical stretching of carboxylate group. The absorption peaks at  $1290$  and  $1158\text{ cm}^{-1}$  correspond to the  $-\text{CH}_2-$ . The strong peak at  $820\text{ cm}^{-1}$  is due to the C-H out of plane bending vibration of aromatic ring. The peak at  $492\text{ cm}^{-1}$  may be due

to the strong chemical bond between silver and carboxylate groups [26,27]. From the FT-IR study, it is inferred that the involvement of some of the bioactive molecules like polyphenolic and its analogs play a major role for green synthesis of silver nanoparticles.

**Antibacterial activity:** The antibacterial activity of green synthesized silver nanoparticles was tested against Gram-negative (*Salmonella* sp.) and Gram-positive (*Bacillus subtilis*) bacteria. The zones of inhibition for *Bacillus subtilis* and *Salmonella* sp. in various concentrations of  $50\text{ }\mu\text{L}$ ,  $75\text{ }\mu\text{L}$  and  $100\text{ }\mu\text{L}$  were found to be around 31 mm, 31 mm, 34 mm, 13 mm, 19 mm and 20 mm, respectively. The results indicated both bacteria have shown efficient minimum inhibitory concentrations (MIC) at three different concentrations of green synthesized silver nanoparticles. The diameter of the zone of inhibition was not changed with increasing the concentration of samples. The different inhibition zone was achieved by Gram-negative and Gram-positive, which is due to the binding of silver nanoparticles with the outer membrane of the Gram-negative bacteria. Due to the chelating ability of silver ion with DNA, which destroys bacterial cells [25]. The antibacterial results suggest the green synthesized silver nanoparticles acted moderately antibacterial agents to treat the infectious disease caused by *Salmonella* sp. and *Bacillus subtilis* pathogens (Table-1).

**Catalytic degradation of textile dyes:** The catalytic behaviour of the green synthesized silver nanoparticles has been investigated towards the catalytic degradation of textile dyes. In present work, methylene blue, malachite green and methyl orange were chosen as model dyes.

The addition of a catalytic quantity of the synthesized silver nanoparticles into the dye solution the degradation of the studied dyes (methylene blue, malachite green and methyl orange) in presence of excess  $\text{NaBH}_4$  as hydrogen sources. Herein, silver nanoparticles functioned as an electron sink to

catalytic degradation of the studied dyes. With the addition of 2 mL AgNPs into the dye solution, the decrease of peak intensity was observed. The continuous degradation of the studied dyes was monitored by UV-visible spectral studies. The resulting decrease in absorbance with respect to the time is shown in Fig. 8. The complete mineralization of methylene blue, methyl orange and malachite green was observed within 10, 12 and 22 min time intervals, respectively.

From these catalytic studies, the synthesized silver nanoparticles can be effectively utilized for the degradation of textile

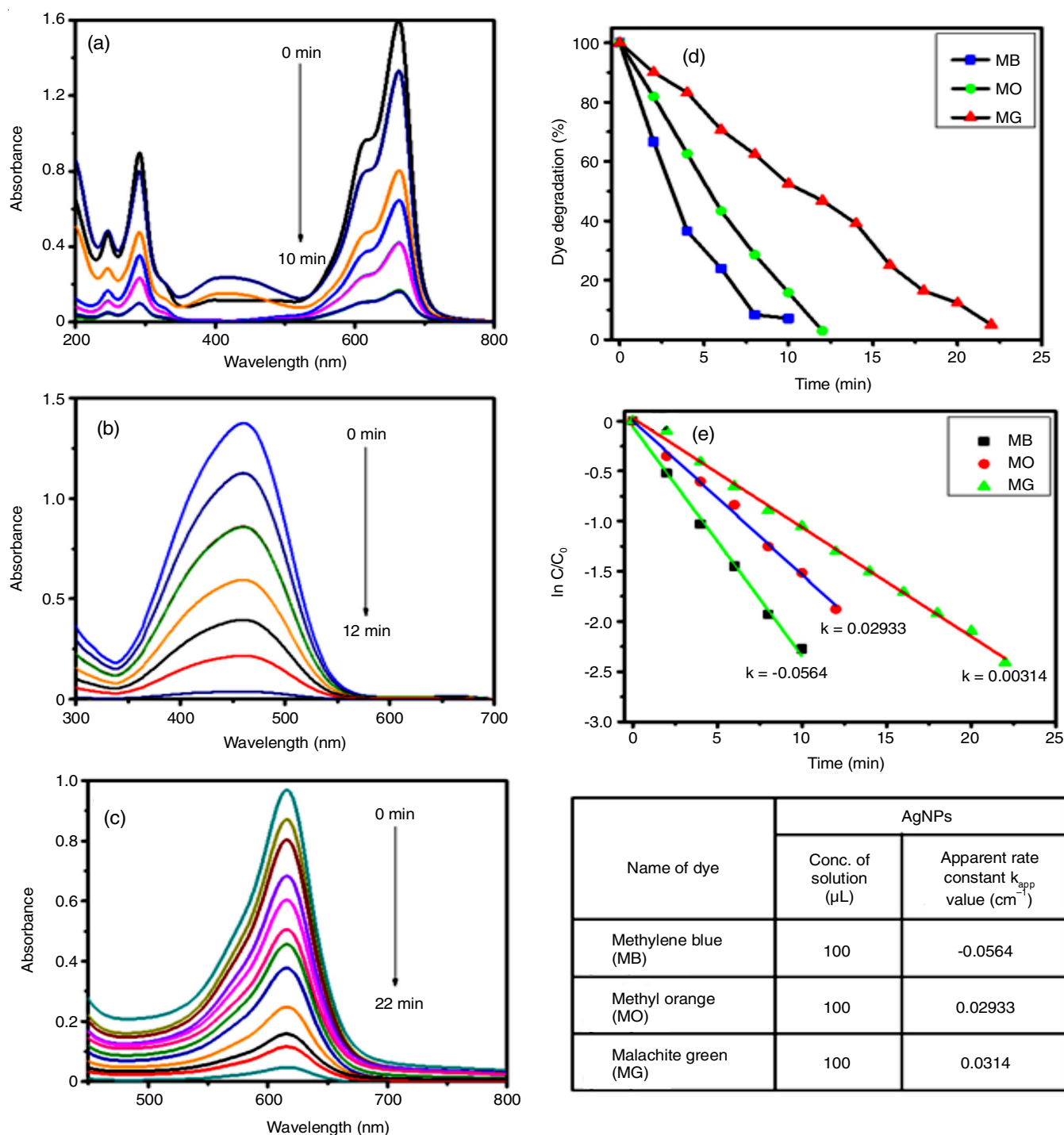


Fig. 8. Catalytic degradation of textile dyes (a) MB, (b) MO, (c) MG, (d) % of dye degradation of MB, MO, MG and (e) The plot of  $\ln(A_0/A_t)$  versus time for the reduction of MB, MO, MG

TABLE-1  
ZONES OF INHIBITION (mm) VALUES AGAINST THE *Bacillus subtilis* AND *Salmonella* sp. FOR SILVER NANOPARTICLES

Name of the samples	Zone of inhibition (mm)							
	Gram-positive bacteria				Gram-negative bacteria			
	<i>Bacillus subtilis</i>				<i>Salmonella</i> sp.			
	A (50 µL)	B (75 µL)	C (100 µL)	D (Std. ampicilin 1 mg/mL)	A (50 µL)	B (75 µL)	C (100 µL)	D (Std. ampicilin 1 mg/mL)
Silver nanoparticles	31	31	34	49	13	19	20	36

TABLE-2  
COMPARISON OF DYE DEGRADATION USING AgNps WITH VARIOUS PLANT MATERIALS

Plant	Dye	Degradation (%)	Time (min)	Reaction rate	Ref.
<i>Medicago polymorpha</i>	Methyl orange	97	5 min	$6.8 \times 10^{-3} \text{ s}^{-1}$	[28]
<i>Calendula officinalis</i>	Methylene blue	>95	40 min	$0.08 \text{ min}^{-1}$	[29]
	Methyl orange	>95	10 min	$0.18 \text{ min}^{-1}$	
<i>Imperata cylindrica</i>	Methylene blue	92	14 min	$0.137 \text{ min}^{-1}$	[30]
<i>Polygonum hydropiper</i>	Methylene blue	–	15 min	–	[31]
<i>Spicy Jatropa</i>	Malachite green	–	30 min	$1.775 \text{ s}^{-1}$	[32]
<i>Thymbra spicata</i>	Methylene blue	–	–	$8.64 \times 10^{-2} \text{ s}^{-1}$	[33]
<i>Mussaenda glabrata</i>	Methyl orange	–	–	$0.7910 \text{ min}^{-1}$	[34]
<i>Mussaenda erythrophylla</i>	Methyl orange	>50	45 min	–	[35]
<i>Terminalia arjuna</i>	Methylene blue	93.60	--	$0.138 \text{ min}^{-1}$	[36]
	Methyl orange	86.68		$0.166 \text{ min}^{-1}$	
<i>Ipomoea quamoclit L.</i>	Methylene blue	>95	10 min	$0.0564 \text{ min}^{-1}$	Current study
	Methyl orange	>95	12 min	$0.02933 \text{ min}^{-1}$	
	Malachite green	>95	23 min	$0.00314 \text{ min}^{-1}$	

dyes from effluent. The comparison of degradation efficacy of silver nanoparticles synthesized by various plant materials is also illustrated in Table-2 [28-36]. Thus, the synthesized AgNPs from *Ipomoea quamoclit* leaf extract is highly stable and can be used as efficient catalyst for decolorization of dyes (methylene blue, malachite green and methyl orange) as compared to other plant materials.

## Conclusion

In present study, the silver nanoparticles were synthesized using *Ipomoea quamoclit* L. leaf extract as the reducing and capping agent. The adopted method was a simple, eco-friendly, fast and efficient method for the green synthesis of silver nanoparticles. Silver nanoparticles with a particle size range around 32 nm were achieved by using *Ipomoea quamoclit* L. and silver nitrate solution at room temperature. The capping and stabilizing agents such as proteins, aromatic compounds and phenols present in the synthesized silver nanoparticles were confirmed by FT-IR spectra and UV-visible spectroscopy. The synthesized silver nanoparticles also exhibited a moderate antibacterial activity against tested bacteria (*Bacillus subtilis* and *Salmonella* sp.).

## CONFLICT OF INTEREST

The authors declare that there is no conflict of interests regarding the publication of this article.

## REFERENCES

- J. Singh, T. Dutta, K.H. Kim, M. Rawat, P. Samddar and P. Kumar, *Nanobiotechnology*, **16**, 84 (2018); <https://doi.org/10.1186/s12951-018-0408-4>
- M. Daniel and D. Astruc, *Chem. Rev.*, **104**, 293 (2004); <https://doi.org/10.1021/cr030698+>
- P. Kurhade, S. Kodape and R. Choudhury, *Chem. Pap.*, **75**, 5187 (2021); <https://doi.org/10.1007/s11696-021-01693-w>
- M.S. Chavali and M.P. Nikolova, *SN Appl. Sci.*, **1**, 607 (2019); <https://doi.org/10.1007/s42452-019-0592-3>
- M. Sebastian, A. Aravind and B. Mathew, *Nanotechnology*, **29**, 355502 (2018); <https://doi.org/10.1088/1361-6528/aac9a>
- A. Rostami-Vartooni, M. Nasrollahzadeh and M. Alizadeh, *J. Colloid Interface Sci.*, **470**, 268 (2016); <https://doi.org/10.1016/j.jcis.2016.02.060>
- B. Wiley, Y. Sun and Y. Xia, *Acc. Chem. Res.*, **40**, 1067 (2007); <https://doi.org/10.1021/ar7000974>
- H.K. Kiranda, R. Mahmud, D. Abubakar and Z.A. Zakaria, *Nanoscale Res. Lett.*, **13**, 1 (2018); <https://doi.org/10.1186/s11671-017-2411-3>
- L.M. Liz-Marzán, *Mater. Today*, **7**, 26 (2004); [https://doi.org/10.1016/S1369-7021\(04\)00080-X](https://doi.org/10.1016/S1369-7021(04)00080-X)
- J. Huang, Q. li, D. Sun, Y. Lu, Y. Su, X. Yang, H. Wang, Y. Wang, W. Shao, N. Her, J. Hong, C. Chen, *Nanotechnology*, **18**, 105104 (2018); <https://doi.org/10.1088/0957-4484/18/10/105104>
- J. Lu, Y. Wang, M. Jin, Z. Yuan, P. Bond and J. Guo, *Water Res.*, **169**, 115229 (2020); <https://doi.org/10.1016/j.watres.2019.115229>
- N. Thangaraju, R.P. Venkatalakshmi, A. Chinnasamy and P. Kannaiyan, *Nano Biomed. Eng.*, **4**, 89 (2012); <https://doi.org/10.5101/nbe.v3i1.p89-94>
- H. Hiramatsu and F.E. Osterloh, *Chem. Mater.*, **16**, 2509 (2004); <https://doi.org/10.1021/cm049532v>
- A. Nirmala Grace and K. Pandian, *Mater. Chem. Phys.*, **104**, 191 (2007); <https://doi.org/10.1016/j.matchemphys.2007.03.009>
- S.P. Chandran, M. Chaudhary, R. Pasricha, A. Ahmad and M. Sastry, *Biotechnol. Prog.*, **22**, 577 (2006); <https://doi.org/10.1021/bp0501423>
- O.V. Kharissova, H.V.R. Dias, B.I. Kharisov, B.O. Pérez and V.M.J. Pérez, *Trends Biotechnol.*, **31**, 240 (2013); <https://doi.org/10.1016/j.tibtech.2013.01.003>
- S. Paul and A. Roychoudhury, *Tropical Plant Res.*, **3**, 616 (2016); <https://doi.org/10.22271/tpr.2016.v3.i3.082>

18. B.A. Fahimmunisha, R. Ishwarya, M.S. AlSalhi, S. Devanesan, M. Govindarajan and B. Vaseeharan, *J. Drug Deliv. Sci. Technol.*, **55**, 101465 (2020);  
<https://doi.org/10.1016/j.jddst.2019.101465>
19. M. Kathirvel, K. Pasupathi, S. Dhamodaran, S. Selvakani and K.G. Mariappan, *Curr. Trends Biotechnol. Pharm.*, **15**, 471 (2021);  
<https://doi.org/10.5530/ctbp.2021.3s.42>
20. M.V. Arularasu, M. Harb and R. Sundaram, *Carbohydr. Polym.*, **249**, 116868 (2020);  
<https://doi.org/10.1016/j.carbpol.2020.116868>
21. E. Parthiban, N. Manivannan, R. Ramanibai and N. Mathivanan, *Biotechnol. Rep.*, **21**, e00297 (2019);  
<https://doi.org/10.1016/j.btre.2018.e00297>
22. H. He, G. Tao, Y. Wang, R. Cai, P. Guo, L. Chen, H. Zuo, P. Zhao and Q. Xia, *Mater. Sci. Eng. C*, **80**, 509 (2017);  
<https://doi.org/10.1016/j.msec.2017.06.015>
23. M.V. Arularasu, *SN Appl. Sci.*, **1**, 393 (2019);  
<https://doi.org/10.1007/s42452-019-0424-5>
24. I. Kubovsky, D. Kacikova and F. Kacik, *Polymers*, **12**, 485 (2020);  
<https://doi.org/10.3390/polym12020485>
25. M.S. Hasnain, M.N. Javed, M.S. Alam, P. Rishishwar, S. Rishishwar, S. Ali, A.K. Nayak and S. Beg, *Mater. Sci. Eng. C*, **99**, 1105 (2019);  
<https://doi.org/10.1016/j.msec.2019.02.061>
26. B. Sadeghi, M. Mohammadzadeh and B. Babakhani, *J. Photochem. Photobiol. B*, **148**, 101 (2015);  
<https://doi.org/10.1016/j.jphotobiol.2015.03.025>
27. F. Nakhjiri and M. Mirhosseini, *Nanomed. J.*, **4**, 98 (2017).
28. M. Ismail, S. Gul, M.I. Khan, M.A. Khan, A.M. Asiri and S.B. Khan, *Green Process. Synth.*, **8**, 118 (2019);  
<https://doi.org/10.1515/gps-2018-0030>
29. S. Chandra Paul, S. Bhowmik, M. Rani Nath, M.S. Islam, S. Kanti Paul, J. Neazi, T. Sabnam Binta Monir, S. Dewanjee and M. Abdus Salam, *Orient. J. Chem.*, **36**, 353 (2020);  
<https://doi.org/10.13005/ojc/360301>
30. A.A. Fairuzi, N. N. Bonnia, R.M Akhir, M.A. Abrani and H.M Akil, *IOP Conf. Ser.: Earth Environ. Sci.*, **105**, 012018 (2018);  
<https://doi.org/10.1088/1755-1315/105/1/012018>
31. N.N. Bonnia, M.S. Kamaruddin, M.H. Nawawi, S. Ratim, H.N. Azlina and E.S. Ali, *Procedia Chem.*, **19**, 594 (2016);  
<https://doi.org/10.1016/j.proche.2016.03.058>
32. P.P. Matheswari, J.I. Jeyamalar and R.N. Asha, *Pharma Innov.*, **8**, 968 (2019).
33. H. Veisi, S. Azizi, P. Mohammadi, *J. Clean. Prod.*, **170**, 1536 (2018);  
<https://doi.org/10.1016/j.jclepro.2017.09.265>
34. S. Francis, S. Joseph, E.P. Koshy and B. Mathew, *Environ. Sci. Pollut. Res. Int.*, **24**, 17347 (2017);  
<https://doi.org/10.1007/s11356-017-9329-2>
35. T. Varadavenkatesan, R. Selvaraj and R. Vinayagam, *J. Mol. Liq.*, **221**, 1063 (2016);  
<https://doi.org/10.1016/j.molliq.2016.06.064>
36. S. Raj, H. Singh, R. Trivedi and V. Soni, *Sci. Rep.*, **10**, 9616 (2020);  
<https://doi.org/10.1038/s41598-020-66851-8>